PLANT SCIENCE TODAY
Vol x(x): xx–xx
https://doi.org/10.14719/pst.11863

eISSN 2348-1900

RESEARCH ARTICLE

Cytotoxic effects of *Juniperus procera* leaf and fruit extracts on human liver cancer cells: *In vitro* and *in silico* evaluation

Ateeq Ahmed Al-Zahrani[1*] & Abdulrahaman M Dogara[2]

[1]Chemistry Department, University College at Al-Qunfudhah, Umm Al-Qura University, Saudi Arabia
[2]Biology Education Department, Tishk International University, Erbil, Iraq

*Correspondence email - aaalzahrani@uqu.edu.sa

Received: 19 September 2025; Accepted: 09 January 2026; Available online: Version 1.0: 16 March 2026

Cite this article: Ateeq AA, Abdulrahaman MD. Cytotoxic effects of *Juniperus procera* leaf and fruit extracts on human liver cancer cells: *In vitro* and *in silico* evaluation. Plant Science Today (Early Access). https://doi.org/10.14719/pst.11863

Abstract

Although there is an increasing body of research focused on natural products for cancer treatment, the therapeutic capabilities of Evaluation of the cytotoxic potential of compounds derived from *Juniperus procera* in diverse liver cell line cultures. especially in terms of a comparative analysis of its leaf and fruit extracts against liver cancer have not been thoroughly investigated. This study offers the first detailed examination that integrates both *in vitro* cytotoxicity assessments and *in silico* molecular modelling to uncover bioactive compounds from *J. procera* with targeted anticancer effects on human liver cancer cells (HepG2). The ethanolic extract from the leaves exhibited significant cytotoxicity (IC_{50} = 17.3 µg/mL), outperforming the fruit extract (IC_{50} = 24.4 µg/mL), while showing low toxicity to normal human fibroblasts (SI > 2). Molecular docking studies targeting mTOR (PDB: 4JT6) revealed Perylene and Podocarpusflavone A as promising high-affinity ligands (ΔG = -10.9 kcal/mol). Quantitative structure-activity relationship (QSAR) modelling, supported by robust statistical validation (Q^2 = 0.649, R^2 = 0.831), indicated that rutin is likely to exhibit the strongest inhibitory effect (IC_{50} = 0.011 nM). Additionally, cytotoxicity predictions using the CLC-Pred tool indicated a broad-spectrum efficacy of selected compounds across various liver cancer cell lines, particularly HepG2. This comprehensive approach underscores the potential of new lead compounds derived from *J. procera* and strongly supports the need for future *in vivo* and target-specific investigations in liver cancer treatment.

Keywords: docking; HepG2; *in vitro–in silico* synergy; *Juniperus procera*; liver cancer; mTOR inhibition; natural products; quantitative structure-activity relationship; rutin

Introduction

Liver cancer poses a significant global health challenge, ranking as the sixth most common cancer and the fourth leading cause of cancer-related mortality worldwide (1). Despite advances in therapeutic approaches including surgical resection, liver transplantation, interventional radiology, localized ablation therapies and targeted immunotherapy outcomes remain suboptimal. Many patients experience high recurrence rates, treatment resistance, or limited access to advanced therapies, leading to persistently low survival rates (2, 3). This underscores the critical need for novel, effective and accessible treatment strategies to improve prognosis for liver cancer patients.

Natural products have long been a cornerstone in drug discovery, particularly for cancer therapeutics. Of the 136 small-molecule anticancer drugs approved to date, 83 % are either natural products or derived from them, with plant-based compounds accounting for nearly half of these agents. Key classes of bioactive plant-derived compounds include alkaloids, flavonoids and terpenoids (4, 5). Among promising plant sources, *Juniperus procera*, a member of the Cupressaceae family, has garnered attention for its rich phytochemical profile. Extracts of *J. procera* have demonstrated diverse pharmacological properties, including antioxidant, antibacterial and anticancer activities, making it a compelling candidate for further investigation (6).

Heterocyclic compounds, particularly those containing nitrogen atoms, are integral to modern medicinal chemistry and anticancer drug development. Notably, 26 of the 40 newly approved molecular antitumor agents incorporate heterocyclic structures and nine of the eleven naturally derived anticancer drugs identified in 2012 were heterocycles (7). These compounds are ubiquitous in nature, with many nitrogen-containing heterocyclic structures found in both traditional remedies and modern pharmaceuticals (8). Their unique chemical properties make them valuable scaffolds for designing targeted anticancer agents.

This study leverages both *in vitro* and *in silico* approaches to evaluate the anticancer potential of *J. procera* extracts and their phytochemical constituents against liver cancer. We hypothesized that *J. procera* leaf and fruit extracts would induce cytotoxic effects in human liver cancer cells and these effects might be mediated by the interaction of certain bioactive compounds with molecular targets relevant for cancer progression, including mTOR signalling pathway as one of key signalling in tumorigenesis. By integrating experimental and computational approaches, the main aims of this work were (i) to evaluate *in vitro* cytotoxic and selectivity potential of *J. procera* extracts against HepG2 cells, (ii) to screen out and

prioritize bioactive-promising phytochemicals based on molecular docking, QSAR modelling as well as ADMET profiling, organ toxicity predictions and drug likeness criteria set by FDA guidelines and (iii) to correlate *in silico* compatibility with *in vitro* assays to propose mechanistic insights fuelling for claimed antiproliferative action. By combining experimental and computational methods, we aim to identify novel therapeutic agents that can address the limitations of current treatments and contribute to the development of more effective strategies for liver cancer management.

Materials and Methods

Plant collection and identification

The fruit and leaf samples of *J. procera* (Fig. 1) were collected from Raghadan forest, which is situated in the Al Bahah Region of the Kingdom of Saudi Arabia. The identification of these plant samples was reported in our previous work (6). The voucher specimens labelled (JPROC-20230115-001) have been preserved in the herbarium of the plant science laboratory at Umm Al-Qura University.

Plant extraction

Approximately 250 g of plant leaves or fruits were subjected to extraction with 96% ethanol three times, each extraction lasting about 48 h and using 2.5 L of ethanol. All extractions were performed at 25 ± 2 ℃, in darkness, with shaking to keep the solution mixed. Following extraction, the solvent was filtered and evaporated using a rotary evaporator. The resulting dried extract was then utilized for further analysis. The residues obtained from the fruit and leaves were then resuspended in methanol (2 mg/mL), preserved at -20 ℃ and applied in subsequent analyses.

Preparation of cell lines

The liver cancer cell line HepG2 and the noncancerous human skin fibroblast cells (HSF) were acquired from Nawah Scientific Company, Egypt. The HSF cells were cultivated in DMEM (Dulbecco's Modified Eagle's Medium) medium (BioWhittaker™). Doxorubicin was procured from Sigma-Aldrich and dissolved in dimethyl sulfoxide (DMSO, Cat. No. 20385.02, Serva, Heidelberg, Germany) before being stored at -20 ℃. The cells were incubated at 37 ℃ in a 5 % CO_2 atmosphere. The extracts were prepared in DMSO (20 mg/mL stock) and stored at -20 ℃.

MTT assay for cell viability

Cell viability was assessed using a method described by previous researchers (9). In brief, the antiproliferative effects of fruit or leaf extracts on HepG2 cells were evaluated. The MTT (3-(4,5-dimethylthiazol-2-yl)-2,5-diphenyltetrazolium bromide) formazan dye was dissolved in DMSO and measured using a plate reader (Biotek, Gen5™) at λ570–630 nm. Initially, 100 µL of cells were plated in a 96 well plate at a density of 5×10^3 cells per well and incubated for 12 hr at 37 ℃ with 5 % CO_2. Subsequently, 200 µL of each extract (100 µg/mL) or DMSO (0.5 % V/V) was added to the wells, followed by another 48 hr incubation under the same conditions. Then, 10 µL of MTT (5 mg/mL in phosphate buffered saline) was added to each well (final MTT concentration of 0.5 mg/mL per well) and the plates were incubated for 4 hr. The formazan crystals were dissolved in 200 µL of 10 % SDS (Sodium dodecyl sulphate) solution (containing 0.01N HCl in 1x PBS, phosphate-buffered saline) after 4 hr of incubation, the absorbance was measured at λ570–630 nm using a plate reader (Biotek, Gen5™). To determine the IC_{50} (Half-maximal inhibitory concentration), cancer cells were exposed to various concentrations of fruit or leaf extracts (5, 10, 20, 50, 100, 200, 500 µg/mL) for 48 hr, followed by MTT assay as described earlier. Doxorubicin was solubilized in sterile deionized water to create a stock solution with a concentration of 1 mg/mL. Subsequently, serial dilutions were conducted to achieve the necessary concentrations, which varied from 0.5 to 20 µg/mL for the assay. All experiments were conducted in triplicate and the results were expressed as mean ± SD of the three measurements in µg/mL.

Screening for selective anticancer activity of the two extracts

The HSF were utilised to assess the selectivity of *Juniperus* fruits and leaves extracts against cancerous cell lines. The cells were cultured in a 96-well plate and left to incubate overnight at 37 ℃ with 5 % CO_2. Subsequently, varying concentrations of the fruit and leaf extracts (5, 10, 20, 50, 100, 200, 500 µg/mL) were introduced to the cells, followed by another round of incubation for 48 hr. Cell viability was then determined using the MTT assay.

Fig. 1. The *Juniperus procera* tree inhabits the Raghadan forest. The aerial parts of the tree are represented on the right, the leaves and fruits displayed on the left (source author). The images were captured using a digital camera, featuring a resolution of 12 megapixels in a "wide" format, complemented by an aperture of f/1.8.

The selectivity index (SI) was calculated using the formula provided earlier (10).

$$\text{Selectivity index (SI)} = \frac{IC_{50}\ \text{normal cells}}{IC_{50}\ \text{cancer cells}}$$

Statistical analysis

The statistical analysis was done through GraphPad Prism version 8.0.2 (GraphPad Software, San Diego, CA, USA). The data are provided in the form of mean ± standard deviation (SD). Each treatment was independently repeated 3 times (biological replicates) and all treatments were done in triplicate well (technical replicates). One way analysis of variance was used to compare groups and then proper post hoc tests were completed, as necessary. A nonlinear regression analysis was done with a four-parameter logistic (variable slope) model and the values of IC_{50} were estimated and the 95 % confidence intervals (95 % CI) were obtained and reported. A *p*-value less than 0.05 was taken as significant.

To enhance the clarity of the methodology, the schematic workflow diagram (Supplementary Fig. 1) with a description of the experimental (extraction, cytotoxicity assays), computational (docking, QSAR, ADMET) steps has been provided.

Molecular docking

The crystal structure of mammalian target of human rapamycin (mTOR) (PDB code: 4JT6) was downloaded from protein data bank (PDB). The native ligand, X6K found in 4JT6 structure and 124 phytochemicals of *J. procera* were obtained from PubChem Search database as canonical smiles strings. The smiles strings were converted to pdb files by a web server called CORINA (11). The ligand input files are automatically optimized by the CB-Dock server, as reported previously (12). CB-Dock is a tool for protein-ligand interactions that detects binding sites, determines their centre and size, adjusts the docking box dimensions based on the query ligands and conducts molecular docking using AutoDock Vina software v1.2 (13). The docking process involves three steps: Search Cavities, View Results and BlindDock. The active site parameters for docking included a Cavity Volume of 2297 Å3, with the centre coordinates of X = 62, Y = -3, Z = -42. The 4JT6 pdb structure consists of four distinct chains: A, B, C and D. To docking, only chain A was employed, rendering the other chains unnecessary and repetitive. The generated poses were evaluated and visualized using the CB-Dock server and Chimaera software tools (14). The inhibition constant (11) was calculated using the formula: $Ki=\exp(\Delta G/RT)$, where ΔG is the binding energy, R is the universal gas constant (1.985×10^{-3} kcal $mol^{-1}K^{-1}$) and T is the temperature (298.15 K).

QSAR study

Dataset preparation

The dataset was created by accessing the Binding DB database, which can be found at https://www.bindingdb.org/rwd/bind/index.jsp. A search was performed using the term "rapamycin (mTOR)" resulting in a total of 380 assays. From this list, one assay was chosen, which included 35 compounds (15), each linked to its corresponding IC_{50} activity as detailed in Supplementary Table 1. The option to “select Affinity Data for This Assay” was utilized, followed by the selection of “Make Data Set.” Ultimately, the compounds were downloaded in a 2D SD file format. These 35 compounds were then imported into ChemMaster 1.2 software, accessible at https://crescent-silico.com/chemmaster/, to develop a QSAR model. The IC_{50} values, measured in nM, were converted to pIC_{50} in molar concentration using the specified equation:

$$-\log(IC50(nM)*10^{**}-9)$$

The pIC_{50} is defined as the negative logarithm of the IC_{50} value, which indicates the concentration required for half-maximal inhibition. Implementing a scaling process is beneficial for improving the linear relationship between biological activity, IC_{50} and various descriptors. Furthermore, this scaling procedure aids in minimizing the variability observed in IC_{50} values.

Data splitting

The dataset was divided into a training set and a test set, with 75 % of the data designated for the training set through the application of K-Means Clustering. The training set serves the purpose of fitting the model, whereas the test set is used for validating the model's performance. K-means clustering is recognized as an effective technique for achieving well-segmented data (16).

The process of constructing a QSAR model involves three essential steps. Initially, the variables x and y were established, with pIC_{50} values designated as the y variable. For the x variable, a range of descriptors related to basic drug-like properties, charge, counts and functional groups were employed, for instance, molecular weight, exact molecular weight, heavy atoms molecular weight, octanol-water partition coefficient (log P), molar refractivity (17), hydrogen bond acceptors, hydrogen bond donors, rotatable bonds, quantitative estimation of drug likeness, maximum partial charge, minimum partial charge, maximum absolute partial charge and minimum absolute partial charge. The second step involved identifying the previously generated divided dataset. Finally, the QSAR model was developed utilizing multiple linear regression (MLR) to evaluate the linear relationship between pIC_{50} and the selected descriptors. A variance threshold of 0.0010 was applied and the sequential feature selection was configured with forward direction, a feature count of 8, k-Fold cross validation set to 4 and RMSE as the evaluation metric. Ultimately, only 8 of the previously mentioned descriptors were utilized in the model, specifically, MR (Molecular refractivity), Minimum Partial Charge, Heavy Atom Count, Num Saturated Heterocycles, Num Saturated Rings, NH0, aniline, ether.

Model validation

The QSAR model developed underwent validation through various parameters calculated separately for the training and test sets. The cross-validated correlation coefficient (Q^2) was employed exclusively for the training set, with a minimum acceptable threshold of ≥ 0.5. The squared correlation coefficient (R^2) was utilized to assess both the training and test sets, with thresholds set at ≥ 0.6 for the training set and ≥ 0.5 for the test set. Additionally, the root mean square error (RMSE) was applied to evaluate both sets, where a lower RMSE indicates a better model. The mean absolute error (MAE) was also used for validation of the training and test sets, with a lower MAE signifying a better model performance.

Virtual screening

Out of the 124 phytochemicals identified from *J. procera* (Supplementary Table 2), 20 compounds were selected for virtual screening. This selection was based on a docking score exceeding -8 kcal/mol, as detailed in Supplementary Table 2. The 20 compounds were sourced from the PubChem database in SDF format and

compiled into a single Text Document file to create a dataset. This dataset was subsequently imported into ChemMaster 1.2 software. The previously established QSAR model was utilized to predict the IC_{50} values for the 20 compounds. The results are presented in molar concentration; therefore, the following equation was used for conversion to nM:

10**-Predicted Ic50 * 10** 9

Prediction of anticancer activity

The evaluation of anticancer efficacy included an analysis of the cytotoxic characteristics of the 20 compounds derived from *J. procera* using CLC-Pred server (Cell Line Cytotoxicity Predictor, version 2.0). This computational tool leverages experimental data to evaluate the cytotoxic effects of the compounds on different colon cancer cell lines. The compounds were input into the server in SMILES format, ensuring that the Pa value was greater than 0.1. The Pa value is a scale that ranges from zero, indicating a lack of activity, to one, which signifies full activity. To visually illustrate the anticancer activity data, a heatmap was generated using Python (version 3.x), available at: https://www.python.org/. This visualization employed the Matplotlib and Seaborn libraries. The data were organized in a tabular format with the help of Pandas, which allowed for the effective display of the anticancer properties of various compounds across multiple liver cancer cell lines.

Evaluation of ADMET

ADMET (Absorption, distribution, metabolism, excretion and toxicity) prediction according to Lipinski's rule of five (RO5) was conducted for each ligand through the SwissADME web server (18).

Results

Cell viability and selective anticancer activity

The anticancer evaluation was conducted using the liver cancer cell line HepG2. The results indicated a greater cytotoxic effect of the leaf extract compared to the fruit extract on HepG2 cells. Specifically, the leaf extract exhibited a cytotoxicity with an IC_{50} value of 17.3 µg/mL, which was more potent than the IC_{50} of the fruit extract, recorded at 24.4 µg/mL (Fig. 2). Additionally, both extracts were assessed for their effects on non-cancerous HSF cells. Neither extract demonstrated significant cytotoxicity, with IC_{50} values of 78.9 µg/mL for the leaf extract and 92.6 µg/mL for the fruit extract (Fig. 3). In this investigation, the IC_{50} value of Doxorubicin for HepG2 cells was determined to be 2.6 µg/mL, while for HSF cells, it was found to be 10 µg/mL. Moreover, both the fruit and leaf extracts exhibited a higher selectivity for cancer cells compared to normal cells, as indicated by a selectivity index (SI) greater than 2.

Following the *in vitro* experiments, an *in silico* analysis was executed on 124 phytochemicals obtained from *J. procera* (Arar) to determine the exact compounds that may function as potential inhibitors of cancer.

Molecular docking analysis

The significant cytotoxic effects observed in the plant extracts prompted us to undertake a comprehensive investigation of the isolated phytochemicals as potential anticancer agents through an *in-silico* approach. To validate the docking procedure utilized by the CB-Dock server, the co-crystallized ligand (X6K) was extracted from the binding site of the human rapamycin structure (PDB: 4JT6). The server successfully re-docked the isolated ligand into the active site of mTOR, demonstrating a close alignment with the original co-crystallized X6K. This alignment serves to confirm the accuracy of the docking protocol (Fig. 4A).

The chemical constituents of *J. procera* and their docking scores against the Human mTOR are detailed in supplementary Table 2. From this analysis, 20 compounds with a binding affinity lower than -8 kcal/mol were selected for further *in silico* studies, which included QSAR modelling and predictions of cytotoxicity. Table 1 provides an overview of the docking scores and inhibition constants for these 20 phytochemicals from *J. procera*. Among these, Perylene and Podocarpusflavone A were found to possess the highest binding affinities of -10.9 kcal/mol. Fig. 4B illustrates the interaction contacts between Perylene and mTOR, specifically LEU2185 LYS2187 TYR2225 ILE2237 GLY2238 TRP2239 VAL2240 MET2345 LEU2354 ILE2356 ASP2357 residues.

QSAR analysis

Numerous efforts were undertaken to construct a QSAR model that effectively characterizes the biological activity of 20 phytochemicals derived from *J. procera*. Various training and testing datasets were generated through both random and

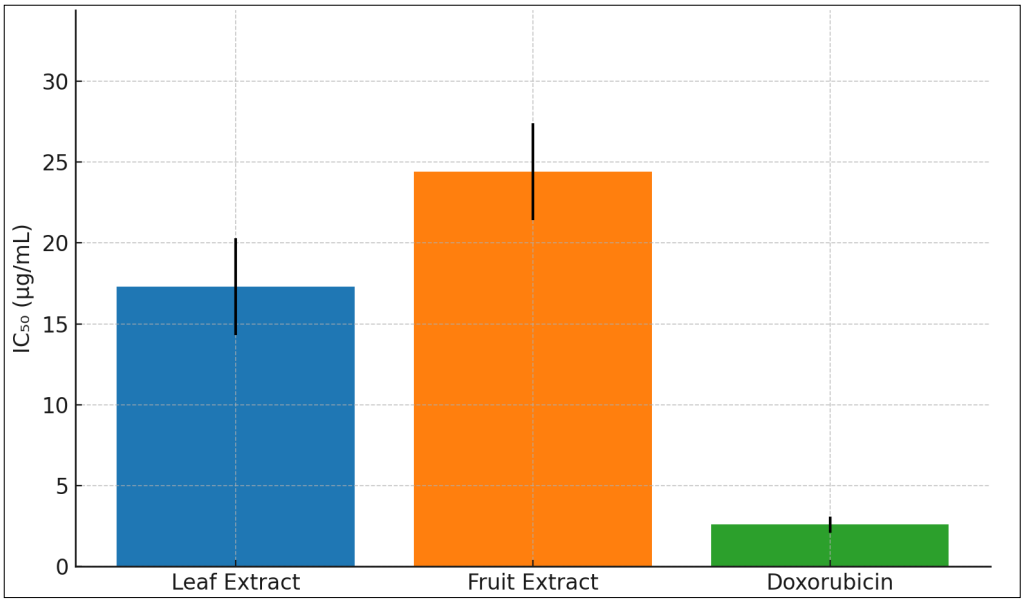

Fig. 2. IC_{50} values of the fruit and leaf extracts for anticancer activity against HepG2 cells.

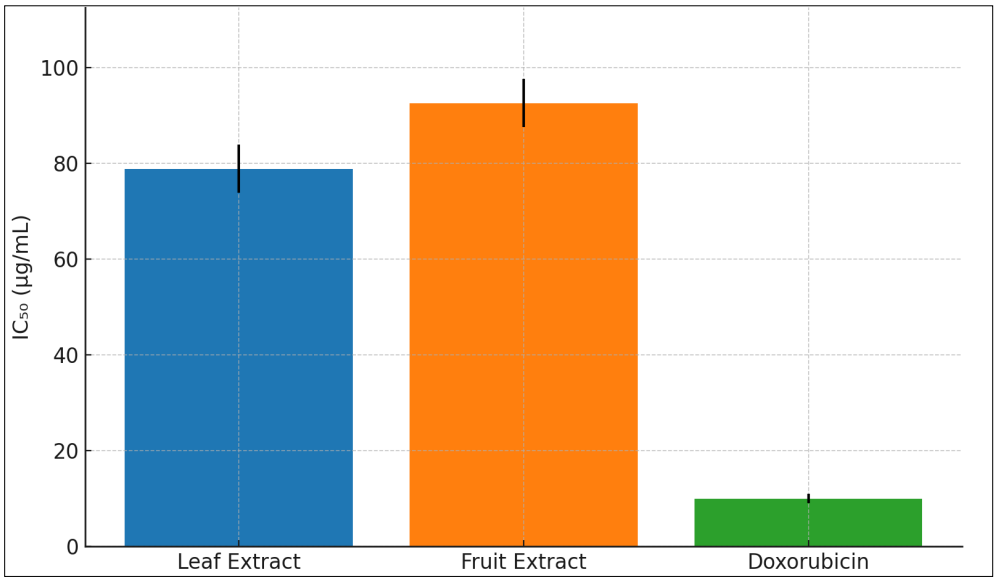

Fig. 3. IC_{50} values of the fruit and leaf extracts for anticancer activity against HSF cells.

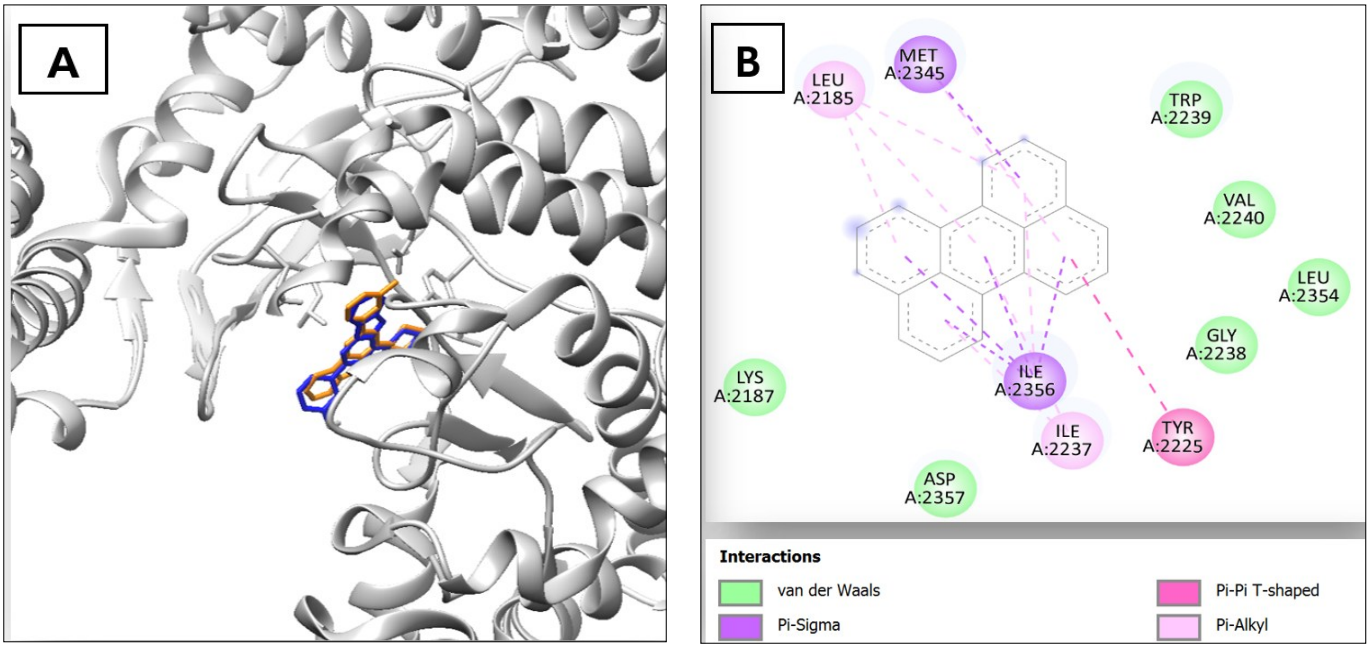

Fig. 4. Validation of the docking protocol and interaction analysis of Perylene with mTOR. A- The validation of the docking protocol, which displays the co-crystallized ligand in orange, the redocked ligand in blue and a portion of mTOR in gray. B- The interaction contacts between mTOR and Perylene.

Table 1. The docking scores and virtual screening results of the 20 phytochemicals of *Juniperus procera* and the positive control, X6K

Compound	PubChem CID	Predicted IC_{50} (31)	Docking Score kcal/mol	Inhibition Constant µM
X6K (Co-crystalized ligand)	9884685	133.8	-9.8	0.061
The 20 phytochemicals of *J. procera*				
Perylene	9142	11.17	-10.9	0.009
Podocarpusflavone A	5320644	0.018	-10.5	0.018
Rutin	5280805	0.011	-9.1	0.200
Quercetin	5280343	5.4	-9.0	0.237
2-Phenanthrenol	69061	1723.4	-8.8	0.333
Juniperolide	101552747	10.9	-8.5	0.554
S-Indacene-1,7-dione	622870	12.5	-8.4	0.656
9(1H)-Phenanthrenone	20531454	85.1	-8.4	0.656
Androstadienone	92979	45.8	-8.4	0.656
1Phenanthrenecarboxaldehyde	11694869	54.7	-8.3	0.777
Isopimara-7(8),15-dien-19-oic acid	442048	211.5	-8.3	0.777
Abietatriene	6432211	13.2	-8.3	0.777
Prasterone	5881	68.4	-8.2	0.920
Dehydroabietic acid	94391	151.8	-8.2	0.920
Sugiol	94162	220.8	-8.1	1.091
alpha-Eudesmol	92762	638.4	-8.1	1.091
Ferruginol	442027	692.6	-8.0	1.292
beta-Eudesmol	91457	834.8	-8.0	1.292
Abieta-7,13-diene	443470	17.7	-8.0	1.292
Epicatechin	72276	4.97	-8.0	1.292

manual sampling techniques. The most suitable QSAR model was identified by evaluating the estimation metrics of Q^2, R^2, RMSE and MAE. A QSAR model was developed utilizing multiple linear regression (MLR) to assess the linear correlation between pIC_{50} and the corresponding descriptors. The construction of the MLR-QSAR model incorporated 8 features, as specified in the methods section. The evaluation of the QSAR model was performed through internal validation with the training set and external validation with the test set. The model passed the statistical quality assessment with a Q^2 of 0.649, R^2 values of 0.831 for the training set and 0.831 for the test set, RMSE values of 0.168 for training and 0.164 for testing and MAE values of 0.136 for training and 0.119 for testing. A significant correlation was observed between the experimental pIC_{50} values and the predicted pIC_{50} values generated by the QSAR model, as demonstrated in Fig. 5. The residuals, calculated by subtracting the experimental pIC_{50} values from the predicted pIC_{50} values, were found to be nearly zero. Consequently, it can be inferred that the QSAR model exhibits strong predictive capability, as indicated in Supplementary Table 1. The MLR-QSAR model produced the following equation that describes the relationship between biological activity (IC_{50}) and the corresponding descriptors.

Equation:

pIC_{50} = -0.9897 * MR +0.1964 * Minimum Partial Charge +1.2267 * HeavyAtomCount -0.0666 * NumSaturatedHeterocycles -0.0666 * NumSaturatedRings -0.2988 * NH0 +0.1932 * aniline +0.1085 * ether +9.1319

The correlation analysis revealed that the Heavy Atom Count exerted the most obvious positive effect on the calculated activity, as evidenced by a coefficient of +11.2267. In contrast, the Molecular Refractivity demonstrated the most considerable negative effect on the calculated activity, reflected by a coefficient of -0.9897. Thus, a higher coefficient value corresponds to a more significant influence on the calculated activity (IC_{50}). The validated MLR-QSAR model was utilized to conduct a virtual screening of 20 phytochemicals derived from *J. procera*, with the objective of identifying potential active inhibitors of the mTOR enzyme. The outcomes of the virtual screening indicated that the compound Rutin exhibited the most favorable IC_{50} value of 0.011 nM, as detailed in Table 1. This value signifies a considerable degree of potent inhibition. Additionally, the compound PodocarpusflavoneA demonstrated a comparable IC_{50} value of 0.018 nM. Overall, all compounds, except for 2-Phenanthrenol, displayed a strong inhibitory effect against mTOR, with IC_{50} values below 1 µM.

Cytotoxic effect of the compounds

An assessment of the anticancer efficacy of 20 compounds was performed using the CLC-Pred server to evaluate their cytotoxic effects on liver cancer cell lines. The outcomes are depicted in Fig. 6, 7 and detailed in Table 2. To ensure the dependability of the predictions, a statistical probability, termed *Pa*, greater than 0.1 was applied. The range of Pa extends from zero, representing no activity, to one, denoting a clear indication of activity. Among the 20 compounds evaluated, 14 exhibited varying degrees of cytotoxicity inhibition against 9 distinct liver cancer cell lines. 2-Phenanthrenol compound displayed the most significant inhibition score of 0.488 against Mahlavu cells. The HepG2 cell line, employed in the *in vitro* investigation, was predicted in the *in-silico* study to be inhibited by 2 compounds, namely Rutin and Podocarpusflavone A, which showed inhibition values of 0.304 and 0.352, respectively.

ADMET of compounds

Evaluating the chemical drug-likeness of compounds is essential for the identification of promising drug candidates, which in turn helps to reduce the financial burden linked to biological and clinical testing. The suitability of all 20 phytochemicals for oral pharmaceutical application in humans was evaluated, following the parameters set by Lipinski's rule of five (RO5). Among these compounds, 19 successfully adhered to the established criteria, with only one violation in some compounds. One violation does not undermine the potential efficacy of these compounds as drugs. Rutin was the only compound that did not comply with Lipinski's rules, exhibiting three violations: a molecular weight

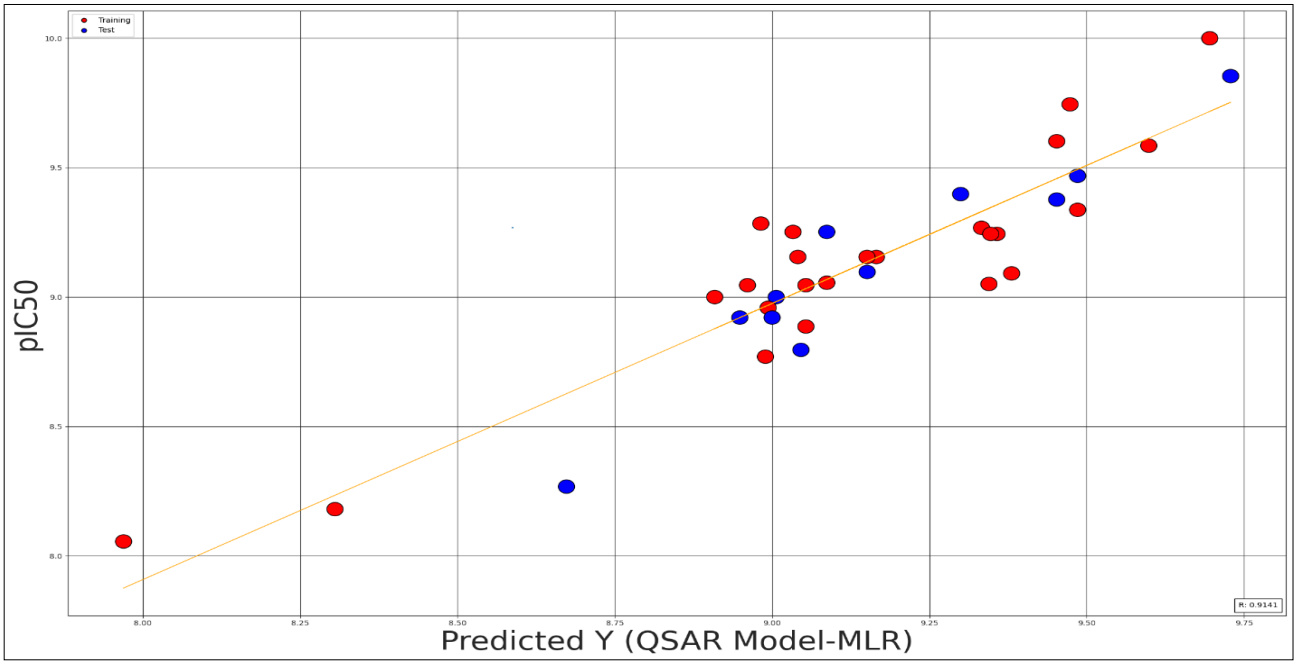

Fig. 5. The MLR-QSAR linear regression model forecasts the inhibitory activity of compounds (Y) based on their experimental inhibitory activity. A closer proximity of the compounds to the Fit line indicates a higher accuracy in predicting their activity. The red circles represent the test dataset, while the blue circles denote the training dataset.

Table 2. The cytotoxic effects of compounds derived from *Juniperus procera* on various liver cancer cell lines. Pa represents the likelihood of a compound being active, while Pi denotes the likelihood of a compound being inactive, based on the training set utilized in the IC_{50} prediction tool. The Pa value (probability of activity) varies from zero, indicating no activity, to one, indicating definite activity. Pa value that >1 was acknowledged in the evaluation

Compound	Pa	Pi	Liver cancer cell lines
Perylene	0.362	0.092	SNU-475 (Hepatocellular carcinoma)
	0.347	0.005	Mahlavu (Hepatocellular carcinoma)
	0.125	0.026	Bel-7402 (Hepatoma)
	0.119	0.024	HA22T (Hepatocellular carcinoma)
Podocarpusflavone A	0.352	0.107	SNU-475 (Hepatocellular carcinoma)
	0.291	0.136	HepG2 (Hepatoblastoma)
	0.285	0.072	PLC-PRF-5 (Hepatocellular carcinoma)
	0.248	0.019	Mahlavu (Hepatocellular carcinoma)
Rutin	0.304	0.188	SNU-475 (Hepatocellular carcinoma)
	0.275	0.102	PLC-PRF-5 (Hepatocellular carcinoma)
	0.249	0.164	HepG2 (Hepatoblastoma)
Quercetin	0.314	0.026	PLC-PRF-5 (Hepatocellular carcinoma)
	0.233	0.024	Mahlavu (Hepatocellular carcinoma)
	0.488	0.002	Mahlavu (Hepatocellular carcinoma)
2-Phenanthrenol	0.381	0.070	SNU-475 (Hepatocellular carcinoma)
	0.273	0.110	PLC-PRF-5 (Hepatocellular carcinoma)
	0.128	0.017	HA22T (Hepatocellular carcinoma)
	0.120	0.030	Bel-7402 (Hepatoma)
Juniperolide	0.326	0.147	SNU-475 (Hepatocellular carcinoma)
S-Indacene-1,7-dione	N/A	N/A	N/A
9(1H)-Phenanthrenone	0.365	0.088	SNU-475 (Hepatocellular carcinoma)
	0.321	0.021	PLC-PRF-5 (Hepatocellular carcinoma)
	0.284	0.010	Mahlavu (Hepatocellular carcinoma)
	0.161	0.154	SK-HEP1 (Hepatocellular carcinoma)
	0.114	0.038	Bel-7402 (Hepatoma)
Androstadienone	0.182	0.007	SMMC-7721 (Hepatocellular carcinoma)
1Phenanthrenecarboxaldehyde	0.114	0.038	Bel-7402 (Hepatoma)
Isopimara-7(8),15-dien-19-oic acid	N/A	N/A	N/A
Abietatriene	0.266	0.265	SNU-475 (Hepatocellular carcinoma)
	0.119	0.032	Bel-7402 (Hepatoma)
Prasterone	0.215	0.005	SMMC-7721 (Hepatocellular carcinoma)
	0.113	0.039	Bel-7402 (Hepatoma)
Dehydroabietic acid	N/A	N/A	N/A
Sugiol	0.361	0.094	SNU-475 (Hepatocellular carcinoma)
	0.287	0.069	PLC-PRF-5 (Hepatocellular carcinoma)
alpha-Eudesmol	N/A	N/A	N/A
Ferruginol	0.351	0.108	SNU-475 (Hepatocellular carcinoma)
	0.304	0.037	PLC-PRF-5 (Hepatocellular carcinoma)
	0.116	0.036	Bel-7402 (Hepatoma)
beta-Eudesmol	N/A	N/A	N/A
Abieta-7,13-diene	N/A	N/A	N/A
Epicatechin	0.320	0.158	SNU-475 (Hepatocellular carcinoma)
	0.296	0.009	Mahlavu (Hepatocellular carcinoma)
	0.244	0.227	PLC-PRF-5 (Hepatocellular carcinoma)

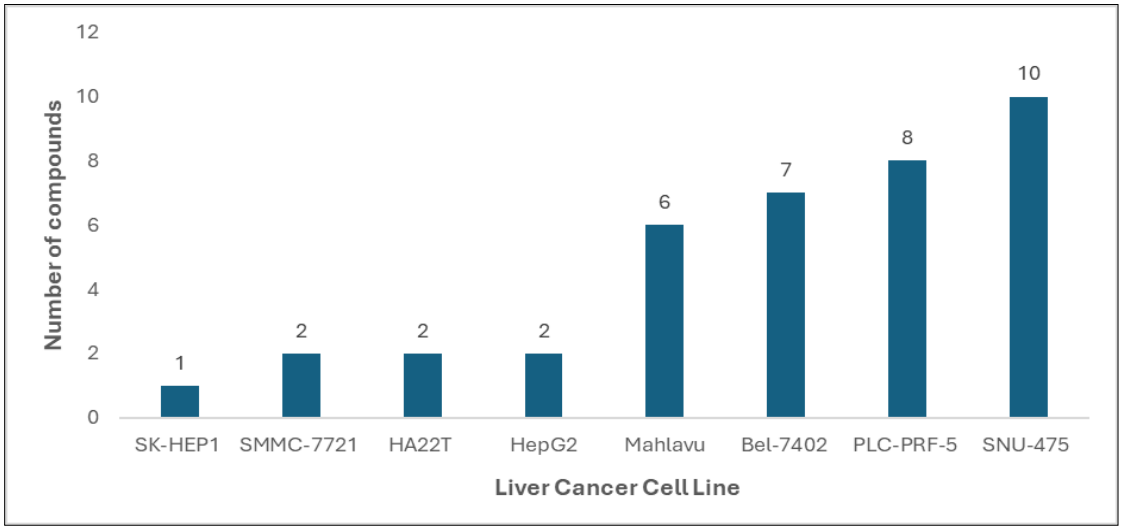

Fig. 6. Evaluation of the cytotoxic potential of compounds derived from *Juniperus procera* in diverse liver cell line cultures.

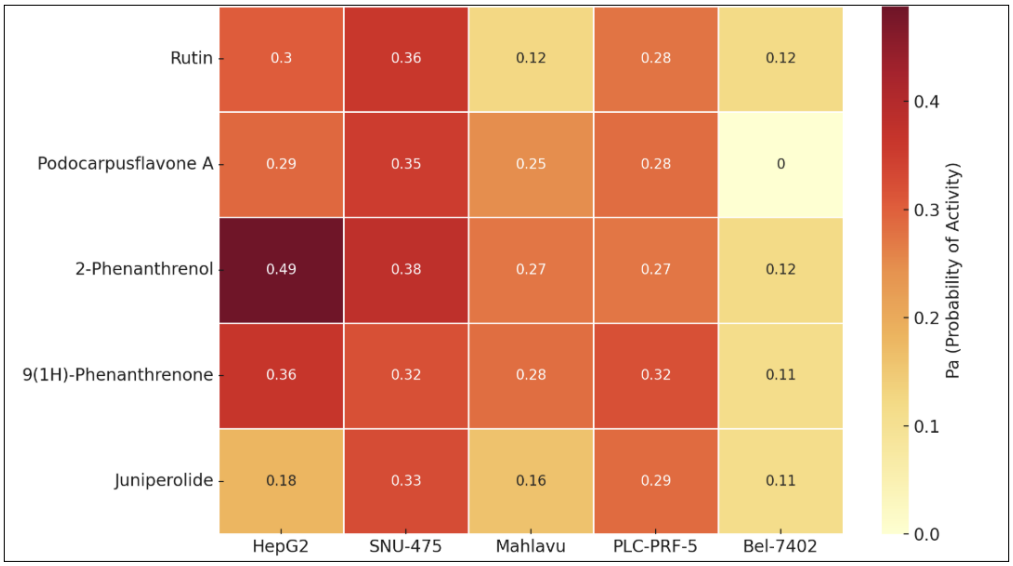

Fig. 7. Heatmap illustrating the maximum Pa values of lead compounds across different liver cancer cell lines. The colour intensity represents the Pa values, with higher values indicating a greater likelihood of activity.

greater than 500, more than 10 rotatable bonds and an excess of 5 hydrogen bond donors or acceptors.

Discussion

The characteristics of the extraction solvents employed play a crucial role in influencing the yield of bioactive compounds, the specific types of compounds that are isolated and the resultant biological activity. In this research, extracts from the leaves and fruits of *J. procera* were obtained utilizing ethanol as the solvent. The obtained residues of these extracts were subsequently resuspended in methanol to improve the solubility of the phytochemicals. The influence of solvent on the yield of extracts in *J. procera* was examined earlier studies (19). Their research indicated that both ethanol and methanol produced the highest yields and optimal recovery of compounds from the seeds and leaves.

This study involved the evaluation of anticancer properties using the HepG2 liver cancer cell line. The results demonstrated that the leaf extract had a significantly stronger cytotoxic impact on HepG2 cells than the fruit extract. The extracts derived from both leaves and fruits in our study exhibited cytotoxic effects on the HepG2 cells, with a high IC_{50} value of 17.3 µg/mL for the leaf extract and a moderate value of 24.4 µg/mL for the fruit extract. The National Cancer Institute (NCI) of the United States classifies the cytotoxicity of a compound based on its IC_{50} values. A compound is considered to exhibit high cytotoxicity when the IC_{50} is less than 20 µg/mL. Moderate cytotoxic activity is observed when the IC_{50} falls between 21 and 200 µg/mL. Weak cytotoxic activity is indicated by an IC_{50} range of 201 to 500 µg/mL, while an IC_{50} greater than 500 µg/mL suggests the absence of cytotoxic activity (20). In a comparable investigation conducted earlier (21), it was reported that the methanolic extract of *J. procera* leaves exhibited a moderate IC_{50} value of 75 µg/mL against HepG2 cells. In contrast, our findings revealed a stronger IC_{50} of 17.3 µg/mL when utilizing ethanolic extracts, suggesting that the ethanolic extracts may contain a higher concentration of anticancer phytochemicals in comparison to the methanolic extract. In comparison to the research conducted by former researchers (22), the ethanolic extract of *J. procera* fruit was subjected to fractionation using a methanolic solvent, which exhibits greater polarity than ethanol. The methanolic fraction demonstrated cytotoxicity with an IC_{50} value of 62.98 µg/mL against HepG2 cells. This finding aligns well with our results, where the fruit extract exhibited moderate cytotoxicity, ranging between 21 and 200 µg/mL. To date, there has been only one study, conducted previously (22), that evaluates the impact of *J. procera* extract on liver cancer cells, specifically concentrating on the fruit extract alone. In contrast, our research examines both fruit and leaf extracts. The limited number of studies on *J. procera* in relation to liver cancer cells emphasizes the critical need for further investigation in this field.

The notable cytotoxic activities presented by the plant extracts inspired us to pursue a thorough investigation of the individual phytochemicals as possible anticancer agents, employing an *in silico* strategy. The constituents of *J. procera* were analyzed via docking studies against the Human mTOR. mTOR was chosen as the molecular target because it plays a central role in the PI3K/Akt/mTOR signalling pathway, which is commonly aberrant in HCC and involved in regulating tumour cell growth, survival and metabolism (23). In addition, mTOR represents an attractive and druggable kinase target since anticancer activity of rapamycin/analogs are demonstrated and the compound-ability of flavonoids to modulate this signalling axis supports the significance of targeting mTOR for phytochemical-based anticancer studies (24).

This analysis led to the identification of 20 compounds that demonstrated a binding affinity lower than -8 kcal/mol, highlighting their potential role as natural inhibitors of mTOR. Research indicates that binding values under -6.0 kcal/mol and occasionally those below -8.0 kcal/mol, are regarded as the most prevalent benchmarks for recognizing potential candidates (25).

Comparison to known mTOR based therapies. Sorafenib, which is a multi-kinase inhibitor, has been put in clinical use as a therapy of advanced hepatocellular carcinoma (HCC) and can also regulate downstream survival signalling and is associated with mTOR-mediated effects (such as autophagy regulation) in HCC models (26). In parallel, rapamycin (sirolimus) and rapalog methods are the standard pharmacologic paradigm of mTOR inhibition; preclinical and translational studies corroborate that mTOR inhibition is capable of suppressing the growth of HCC and has since been widely presented as a therapeutic concept in HCC (27). In this regard, it is expected because the binding of key constituents

(e.g., rutin/Podocarpusflavone A) to mTOR will also be strong, which indicates that *J. procera* phytochemicals can be used as natural mTOR-modulating candidates which will supplement the overall signalling inhibition of sorafenib. The common malregulation of PI3K/AKT/mTOR axis in HCC also justifies the choice of mTOR as a mechanistically important target to be prioritized through computation (28).

The lead compounds investigated in this study were assessed for their possible contributions to liver cancer therapy. The literature revealed that there have been no prior suggestions of Perylene and Podocarpusflavone A compounds as inhibitors of mTOR. Research on perylene derivatives was performed *in vitro* to evaluate their cytotoxic properties against the SK-HEP-1 liver adenocarcinoma, indicating a considerable antiproliferative impact on this specific cell line (29). Perylene exhibits aggregation and stack formation via π–π aromatic interactions within a biological context. The solubility of perylene can be improved by altering the imide positions of its core with hydrophilic biomolecules, which in turn influences its self-assembly for biotechnological applications and its cytotoxic effects on tumor cells (30). Podocarpusflavone A, another compound of interest, has been reported to exhibit cytotoxic properties against various cell lines, including HepG2 cells, which are the cancer cells examined in our research. Analysis of the structure-activity relationship reveals that 'OMe' groups in biflavonoids are essential in facilitating cytotoxicity (31). The compound Rutin, in addition to Podocarpusflavone A, was also predicted in our computational study to exhibit cytotoxic effects against HepG2 cells. The proliferation of HepG2 cells was notably inhibited by rutin, which also induced apoptosis, with effects that were contingent upon the concentration used (32). In previous studies, rutin was found to possess cytotoxic properties against HepG2 cells, achieving an IC_{50} of 50.0 µg/mL (33). Our research revealed that Rutin was the sole compound that failed to adhere to Lipinski's rules due to its inadequate solubility. This limitation was addressed and explored in previous study (17), that incorporated various saturated fatty acids and additional chemicals to enhance the solubility of rutin and improve its cytotoxic effects on human liver cancer cell lines.

Our *in silico* analysis has identified four primary lead compounds: Perylene, Podocarpusflavone A, Rutin and Quercetin. These compounds are classified as heterocyclic compounds. Recently, heterocyclic compounds derived from natural sources have significantly contributed to the development of anticancer pharmaceuticals, both in their native and chemically altered states. Notably, a highly effective strategy for discovering novel anticancer agents involves the chemical modification of naturally occurring substances that exhibit established anticancer efficacy. The years 2010 to 2015 were marked by the fact that over 65 % of anticancer pharmaceuticals sanctioned by the food and drug administration (FDA) featured a heterocyclic ring, emphasizing its crucial importance in the realm of drug development (34). The majority of heterocyclic compounds found in current anticancer medications incorporate a nitrogen atom within their molecular framework, which enhances their ability to trigger apoptosis in cancer cells (35). A synthesis and evaluation of the anti-tumour properties of 16 nitrogen heterocyclic compounds was reported earlier (36). These newly synthesized derivatives were subjected to *in vitro* testing for their anti-proliferative effects on human liver (HepG2) cell line, with their efficacy being benchmarked against Doxorubicin. Notably, compound 2 exhibited remarkable anticancer activity, demonstrating an IC_{50} value of 7.36 µM, in contrast to Doxorubicin's IC_{50} value of 4.5 µM (37).

In conclusion, although it is conceptually reasonable to relate crude-extract cytotoxicity to predicted mTOR inhibitory activity, it should be understood as being proposed rather than established. The studied HepG2 cytotoxic effect can be due to series of mechanism (e.g., oxidative stress balance, mitochondrial effects, apoptotic pathway) or the synergy between several extract compounds rather than one targeted mechanism. Thus, docking/QSAR/ADMET results are to be considered as a triage process (about predicting likely active molecules and pathways that warrant confirmation in future mechanistic assays such as mTOR phosphorylation readouts/pathway reporters/target engagement studies). It is supported by the evidence that in some cases crude plant extracts can exhibit more potent activity than isolated constituents (37).

Conclusion

Presently, there is a renewed focus on naturally occurring compounds with biological properties in developed nations, while the use of medicinal plants continues to be a universally recognized therapeutic approach globally, particularly in less developed areas. The notable *in vitro* findings from the leaf and fruit extracts prompted us to employ *in silico* methodologies to identify potential individual compounds that may function as promising anticancer agents. The novelty of this study is the combined use of *in vitro* cytotoxic assessment with *in silico* molecular docking, QSAR-based modelling and cytotoxicity prediction to pipeline bioactive compounds from *J. procera*. A total of 124 phytochemicals derived from *J. procera* have been documented in the literature, of which 20 compounds displayed significant docking scores of -8 kcal/mol when evaluated against the mTOR enzyme. Perylene exhibited the most significant inhibition score of -10.9 kcal/mol against mTOR. Subsequent investigations utilizing QSAR analysis revealed that Rutin presented the most promising IC_{50} value of 0.011 nM, while Podocarpusflavone A exhibited a similar IC_{50} value of 0.018 nM. Furthermore, the cytotoxicity predictions indicated that out of the 20 compounds assessed, 14 demonstrated varying levels of cytotoxicity inhibition across nine different liver cancer cell lines. The HepG2 cell line utilized in the *in vitro* study was anticipated to be inhibited by two specific compounds identified in the *in-silico* analysis, Rutin and Podocarpusflavone A, which exhibited inhibition values of 0.304 and 0.352, respectively. Nonetheless, one should be cautious when interpreting these results as anticancer activities were observed using crude extracts whereas the involvement of mTOR inhibition was predicted *in-silico* but not yet validated experimentally. Thus, the compounds identified should be considered as initial leads and more target-oriented approaches, mechanisms research and animal models are needed to validate their anticancer activities. Pending the outcomes of clinical trials, the lead compounds are expected to function as prospective pharmaceuticals for the treatment of liver cancer cells.

Authors' contributions

AAA and AMD performed the *in vitro* experiments and AAA conducted the *in silico* study. AAA and AMD carried out the data analysis. Both authors read and approved the final version of manuscript.

Compliance with ethical standards

Conflict of interest: The author declares that there no conflict of interest.

Ethical issues: None

References

1. Peng J, Lue M, Peng Y, Tang X. Global incidence of primary liver cancer by etiology among children, adolescents and young adults. J Hepatol. 2023;79(2):e92-4. https://doi.org/10.1016/j.jhep.2023.02.019
2. Muñoz-Martínez S, Iserte G, Sanduzzi-Zamparelli M, Llarch N, Reig M. Current pharmacological treatment of hepatocellular carcinoma. Curr Opin Pharmacol. 2021;60:141-8. https://doi.org/10.1016/j.coph.2021.07.009
3. Rizzo A, Mollica V, Tateo V, Tassinari E, Marchetti A, Rosellini M, et al. Hypertransaminasemia in cancer patients receiving immunotherapy and immune-based combinations: the MOUSEION-05 study. Cancer Immunol Immunother. 2023;72(6):1381-94. https://doi.org/10.1007/s00262-023-03366-x
4. Man S, Luo C, Yan M, Zhao G, Ma L, Gao W. Treatment for liver cancer: from sorafenib to natural products. Eur J Med Chem. 2021;224:113690. https://doi.org/10.1016/j.ejmech.2021.113690
5. Das AP, Agarwal SM. Recent advances in the area of plant-based anti-cancer drug discovery using computational approaches. Mol Divers. 2024;28(2):901-25. https://doi.org/10.1007/s11030-022-10590-7
6. Al-Zahrani AA, Ibraheem F, El-Hefny M, El-Senduny F. Evaluation of Saudi *Juniperus procera* extracts cytotoxicity and regulatory mechanisms of tumorigenesis against two breast cancer cell lines. Nat Prod Commun. 2024;19(2):1934578X241232778. https://doi.org/10.1177/1934578X241232778
7. Al-Jumaili MHA, Hamad AA, Hashem HE, Hussein AD, Muhaidi MJ, Ahmed MA, et al. Comprehensive review on the bis-heterocyclic compounds and their anticancer efficacy. J Mol Struct. 2023;1271:133970. https://doi.org/10.1016/j.molstruc.2022.133970
8. Negi B, Kwatra A. A review of recent progress on the anticancer activity of heterocyclic compounds. SynOpen. 2024;8(3):185-210. https://doi.org/10.1055/s-0040-1720125
9. Graidist P, Martla M, Sukpondma Y. Cytotoxic activity of *Piper cubeba* extract in breast cancer cell lines. Nutrients. 2015;7(4):2707-18. https://doi.org/10.3390/nu7042707
10. Indrayanto G, Putra GS, Suhud F. Validation of *in vitro* bioassay methods: application in herbal drug research. Profiles Drug Subst Excip Relat Methodol. 2021;46:273-307. https://doi.org/10.1016/bs.podrm.2020.07.005
11. Sadowski J, Gasteiger J, Klebe G. Comparison of automatic three-dimensional model builders using 639 X-ray structures. J Chem Inf Comput Sci. 1994;34(4):1000-8. https://doi.org/10.1021/ci00020a039
12. Dakpa G, Kumar KS, Nelen J, Perez-Sanchez H, Wang SY. Antcin-B, a phytosterol-like compound from *Taiwanofungus camphoratus* inhibits SARS-CoV-2 3-chymotrypsin-like protease activity in silico and *in vitro*. Sci Rep. 2023;13(1):17106. https://doi.org/10.1038/s41598-023-44476-x
13. Eberhardt J, Santos-Martins D, Tillack AF, Forli S. AutoDock Vina 1.2.0: new docking methods, expanded force field and python bindings. J Chem Inf Model. 2021;61(8):3891-8. https://doi.org/10.1021/acs.jcim.1c00203
14. Pettersen EF, Goddard TD, Huang CC, Couch GS, Greenblatt DM, Meng EC, et al. UCSF Chimera: a visualization system for exploratory research and analysis. J Comput Chem. 2004;25(13):1605-12. https://doi.org/10.1002/jcc.20084
15. Verheijen JC, Richard DJ, Curran K, Kaplan J, Yu K, Zask A. 2-Arylureidophenyl-4-(3-oxa-8-azabicyclo[3.2.1]octan-8-yl) triazines as highly potent and selective ATP competitive mTOR inhibitors: optimization of human microsomal stability. Bioorg Med Chem Lett. 2010;20(8):2648-53. https://doi.org/10.1016/j.bmcl.2010.02.031
16. Andrada MF, Vega-Hissi EG, Estrada MR, Martinez JCG. Application of k-means clustering, linear discriminant analysis and multivariate linear regression for the development of a predictive QSAR model on 5-lipoxygenase inhibitors. Chemom Intell Lab Syst. 2015;143:122-9. https://doi.org/10.1016/j.chemolab.2015.03.001
17. AbouSamra MM, Afifi SM, Galal AF, Kamel R. Rutin-loaded phyto-sterosomes as a potential approach for the treatment of hepatocellular carcinoma: *in vitro* and *in vivo* studies. J Drug Deliv Sci Technol. 2023;79:104015. https://doi.org/10.1016/j.jddst.2022.104015
18. Al-Zahrani AA. Aromatase inhibition using *Juniperus procera* phytochemical constituents: molecular docking study. J Umm Al-Qura Univ Appl Sci. 2024;10(3):438-44. https://doi.org/10.1007/s43994-023-00114-w
19. Salih AM, Al-Qurainy F, Nadeem M, Tarroum M, Khan S, Shaikhaldein HO, et al. Optimization method for phenolic compounds extraction from medicinal plant (*Juniperus procera*) and phytochemicals screening. Molecules. 2021;26(24):7454. https://doi.org/10.3390/molecules26247454
20. Damasuri AR, Sholikhah EN. Cytotoxicity of (E)-1-(4-aminophenyl)-3-phenylprop-2-en-1-one on HeLa cell line. Indones J Pharm Ther. 2020;1(2). https://doi.org/10.22146/ijpther.606
21. Alhayyani S, Akhdhar A, Asseri AH, Mohammed AM, Hussien MA, Roselin LS, et al. Potential anticancer activity of *Juniperus procera* and molecular docking models of active proteins in cancer cells. Molecules. 2023;28(5):2041. https://doi.org/10.3390/molecules28052041
22. Alghamdi MD, Nazreen S, Ali NM, Amna T. ZnO nanocomposites of *Juniperus procera* and *Dodonaea viscosa* extracts as antiproliferative and antimicrobial agents. Nanomaterials. 2022;12(4):664. https://doi.org/10.3390/nano12040664
23. Jiang M, Zhang K, Zhang Z, Zeng X, Huang Z, Qin P, et al. PI3K/AKT/mTOR axis in cancer: from pathogenesis to treatment. MedComm. 2025;6(8):e70295. https://doi.org/10.1002/mco2.70295
24. Sabatini DM. mTOR and cancer: insights into a complex relationship. Nat Rev Cancer. 2006;6(9):729-34. https://doi.org/10.1038/nrc1974
25. Ivanova L, Karelson M. The impact of software used and the type of target protein on molecular docking accuracy. Molecules. 2022;27(24):9041. https://doi.org/10.3390/molecules27249041
26. Tang W, Chen Z, Zhang W, Cheng Y, Zhang B, Wu F, et al. The mechanisms of sorafenib resistance in hepatocellular carcinoma: theoretical basis and therapeutic aspects. Signal Transduct Target Ther. 2020;5(1):87. https://

doi.org/10.1038/s41392-020-0187-x

27. Matter MS, Decaens T andersen JB, Thorgeirsson SS. Targeting the mTOR pathway in hepatocellular carcinoma: current state and future trends. J Hepatol. 2014;60(4):855-65. https://doi.org/10.1016/j.jhep.2013.11.031
28. Zheng J, Wang S, Xia L, Sun Z, Chan KM, Bernards R, et al. Hepatocellular carcinoma: signaling pathways and therapeutic advances. Signal Transduct Target Ther. 2025;10(1):35. https://doi.org/10.1038/s41392-024-02075-w
29. Abourajab A, et al. Synthesis, characterization, anti-cancer evaluation and DNA-binding study of new bay-substituted perylene derivatives. J Biol Med. 2023;7(1):031-43. https://doi.org/10.17352/jbm.000039
30. Rostaminejad B, Dinari M, Karimi AR, Hadizadeh M. Oxidative cross-linking of biocompatible chitosan injectable hydrogel by perylene-dopamine to boost phototoxicity of perylene on *in vitro* melanoma and breast cancer therapy. J Mol Liq. 2023;386:122553. https://doi.org/10.1016/j.molliq.2023.122553
31. Menon LN, Sindhu G, Raghu KG, Rameshkumar KB. Chemical composition and cytotoxicity of *Garcinia rubro-echinata*, a Western Ghats endemic species. Nat Prod Commun. 2018;13(11). https://doi.org/10.1177/1934578X1801301121
32. Shen Q, Ma Z, Chen G. Effect of rutin on proliferation of HepG2 cells. J Third Mil Med Univ. 2003.
33. Barcelos GR, Grotto D, Angeli JPF, Serpeloni JM, Rocha BA, Bastos JK, et al. Evaluation of antigenotoxic effects of plant flavonoids quercetin and rutin on HepG2 cells. Phytother Res. 2011;25(9):1381-8. https://doi.org/10.1002/ptr.3436
34. Kerru N, Gummidi L, Maddila S, Gangu KK, Jonnalagadda SB. A review on recent advances in nitrogen-containing molecules and their biological applications. Molecules. 2020;25(8):1909. https://doi.org/10.3390/molecules25081909
35. Sidhu JS, Singla R, Mayank, Jaitak V. Indole derivatives as anticancer agents for breast cancer therapy: a review. Anticancer Agents Med Chem. 2015;16(2):160-73. https://doi.org/10.2174/1871520615666150520144217
36. Ahmed MH, El-Hashash MA, Marzouk MI, El-Naggar AM. Synthesis and antitumor activity of some nitrogen heterocycles bearing pyrimidine moiety. J Heterocycl Chem. 2020;57(9):3412-27. https://doi.org/10.1002/jhet.4061
37. Kumar A, Singh AK, Singh H, Vijayan V, Kumar D, Naik J, et al. Nitrogen containing heterocycles as anticancer agents: a medicinal chemistry perspective. Pharmaceuticals. 2023;16(2). https://doi.org/10.3390/ph16020299
38. Yang H, Rudge DG, Koos JD, Vaidialingam B, Yang HJ, Pavletich NP. mTOR kinase structure, mechanism and regulation. Nature Publishing Group; Nature. 2013;497(7448):217-23. https://doi.org/10.1038/nature12122
39. Muhammad I, Mossa JS, Al-Yahya MA, Ramadan AF, El-Feraly FS. Further antibacterial diterpenes from the bark and leaves of *Juniperus procera* Hochst. ex Endl. Phytotherapy Research. 1995;9(8):584-8. https://doi.org/10.1002/ptr.2650090810
40. Alqasoumi SI, Abdel-Kader MS. Terpenoids from *Juniperus procera* with hepatoprotective activity. Pakistan Journal of Pharmaceutical Sciences. 2012;25(2).
41. Al-Ghamdi AAM, Jais HM, Khogali A. Relationship between the status of arbuscular mycorrhizal colonization in the roots and heavy metal and flavonoid contents in the leaves of *Juniperus procera*. Journal of Ecology and The Natural Environment. 2012;4(8):212-8. https://doi.org/10.5897/JENE12.023
42. Samaha HAM, Ali NAA, Mansi I, Abu-El-Halawa R. Antimicrobial, antiradical and xanthine oxidase inhibitory activities of *Juniperus procera* plant extracts from Albaha. World Journal of Pharmacy and Pharmaceutical Sciences. 2017;6(2):232-42.
43. Almadiy AA. Chemical composition, insecticidal and biochemical effects of two plant oils and their major fractions against *Aedes aegypti*. Heliyon. 2020;6(9):e04915. https://doi.org/10.1016/j.heliyon.2020.e04915
44. Abdelghany TM, Hassan MM, El-Naggar MA, Abd El-Mongy M. GC/MS analysis of *Juniperus procera* extract and its activity with silver nanoparticles against *Aspergillus flavus*. Biotechnology Reports. 2020;27:e00536. https://doi.org/10.1016/j.btre.2020.e00496
45. Salih AM, Al-Qurainy F, Khan S, Tarroum M, Nadeem M, Shaikhaldein HO, et al. Mass propagation of *Juniperus procera* and screening of bioactive compounds. BMC Plant Biology. 2021; 21:1-13. https://doi.org/10.1186/s12870-021-02946-2
46. Abobakr Y, Al-Sarar AS, Abdel-Kader MS. Fumigant toxicity and feeding deterrent activity of essential oils from *Lavandula dentata*, *Juniperus procera*, and *Mentha longifolia*. Agriculture. 2022;12(7):934. https://doi.org/10.3390/agriculture12070934
47. Adams RP. Juniperus procera of East Africa: Volatile leaf oil composition and putative relationship to *J. excelsa*. Biochemical Systematics and Ecology. 1990;18(4):207-10. https://doi.org/10.1016/0305-1978(90)90061-J
48. Kinyanjui T, Gitu PM, Kamau GN. Potential antitermite compounds from *Juniperus procera* extracts. Chemosphere. 2000;41(7):1071-4. https://doi.org/10.1016/S0045-6535(99)00460-9
49. Burits M, Asres K, Bucar F. The antioxidant activity of the essential oils of *Artemisia afra*, *Artemisia abyssinica* and *Juniperus procera*. Phytotherapy Research. 2001;15(2):103-8. https://doi.org/10.1002/ptr.691
50. Samoylenko V, Dunbar DC, Gafur MA, Khan SI, Ross SA, Mossa JS, et al. Antiparasitic, nematicidal and antifouling constituents from *Juniperus* berries. Phytotherapy Research. 2008;22(12):1570-6. https://doi.org/10.1002/ptr.2460
51. Nduati TW, Wagara IN, Walyambillah W, Were B, Matasyoh JC. Bioactive compounds from *Juniperus procera* (Cupressaceae) with activity against common bean bacterial pathogens. African Journal of Biotechnology. 2023;22(6):106-13. https://doi.org/10.5897/AJB2023.17552

Additional information

Peer review: Publisher thanks Sectional Editor and the other anonymous reviewers for their contribution to the peer review of this work.

Reprints & permissions information is available at https://horizonepublishing.com/journals/index.php/PST/open_access_policy

Publisher's Note: Horizon e-Publishing Group remains neutral with regard to jurisdictional claims in published maps and institutional affiliations.

Indexing: Plant Science Today, published by Horizon e-Publishing Group, is covered by Scopus, Web of Science, BIOSIS Previews, Clarivate Analytics, NAAS, UGC Care, etc
See https://horizonepublishing.com/journals/index.php/PST/indexing_abstracting

Publisher information: Plant Science Today is published by HORIZON e-Publishing Group with support from Empirion Publishers Private Limited, Thiruvananthapuram, India.